

AD-A139 297

THE DETECTION OF FAINT SPACE OBJECTS USING SOLID STATE
IMAGING DETECTORS(U) MICHIGAN UNIV ANN ARBOR DEPT OF
PHYSICS D J HEGYI 31 DEC 83 AFOSR-TR-84-0159

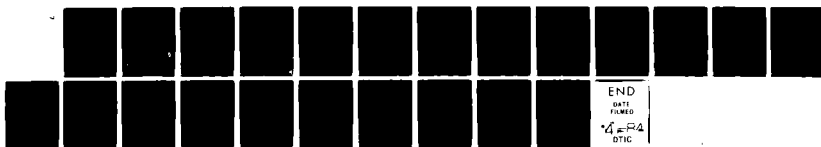
1/1

UNCLASSIFIED

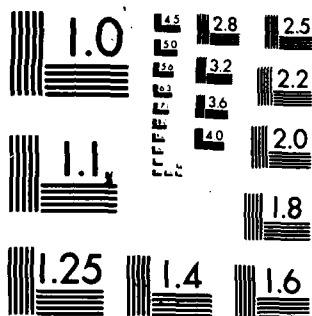
AFOSR-80-0095

F/G 3/1

NL



END
DATE
FILMED
AFOSR
DTIC



MICROCOPY RESOLUTION TEST CHART
NATIONAL BUREAU OF STANDARDS-1963-A

AD A139297

ANNUAL TECHNICAL REPORT: 1/1/83-12/31/83
AFOSR 80-0095

THE DETECTION OF FAINT SPACE OBJECTS USING
SOLID STATE IMAGING DETECTORS

The University of Michigan
Department of Physics
Ann Arbor, MI 48109

DTIC FILE COPY

DTIC
ELECTE
MAR 23 1984
S D
A

Principal Investigator: Dennis J. Hegyi

84 03 22

Approved for public release;
distribution unlimited.
123

UNCLASSIFIED

SECURITY CLASSIFICATION OF THIS PAGE

REPORT DOCUMENTATION PAGE

1a. REPORT SECURITY CLASSIFICATION Unclassified			1b. RESTRICTIVE MARKINGS		
2a. SECURITY CLASSIFICATION AUTHORITY			3. DISTRIBUTION/AVAILABILITY OF REPORT Approved for public release; distribution unlimited		
2b. DECLASSIFICATION/DOWNGRADING SCHEDULE					
4. PERFORMING ORGANIZATION REPORT NUMBER(S)			5. MONITORING ORGANIZATION REPORT NUMBER(S) AFOSR-TR- 84 - 0159		
6a. NAME OF PERFORMING ORGANIZATION University of Michigan		6b. OFFICE SYMBOL (If applicable)		7a. NAME OF MONITORING ORGANIZATION AFOSR	
6c. ADDRESS (City, State and ZIP Code) Department of Physics Ann Arbor, MI 48109				7b. ADDRESS (City, State and ZIP Code) Bldg 410 Bolling AFB, DC 20332	
8a. NAME OF FUNDING/SPONSORING ORGANIZATION AFOSR		8b. OFFICE SYMBOL (If applicable) NP		9. PROCUREMENT INSTRUMENT IDENTIFICATION NUMBER AFOSR-80-0095	
8c. ADDRESS (City, State and ZIP Code) Bolling AFB, DC 20332		10. SOURCE OF FUNDING NOS.			
		PROGRAM ELEMENT NO. 61102F		PROJECT NO. 2311	TASK NO. A1
					WORK UNIT NO.
11. TITLE (Include Security Classification) THE DETECTION OF FAINT SPACE OBJECTS USING SOLID STATE IMAGING DETECTORS					
12. PERSONAL AUTHOR(S) Dennis J. Hegyi					
13a. TYPE OF REPORT Annual		13b. TIME COVERED FROM 1 Jan 83 to 31 Dec 83		14. DATE OF REPORT (Yr., Mo., Day) 31 Dec 83	
				15. PAGE COUNT 22	
16. SUPPLEMENTARY NOTATION					
17. COSATI CODES			18. SUBJECT TERMS (Continue on reverse if necessary and identify by block number)		
FIELD	GROUP	SUB. GR.			
19. ABSTRACT (Continue on reverse if necessary and identify by block number) Speckle interferometry has been carried out during the last year with a charge-coupled device (CCD) imaging system. The emphasis of this project has been to minimize all systematic differences that arise between the images of stars in a binary star system and a reference calibration star in order to resolve a previously unresolved binary star system. Systematic errors have been minimized to the level of parts in 10,000 in the power spectrum of a stellar image. This was accomplished by using a 64x64 pixel area near the readout amplifier to minimize charge smearing, by stabilizing our CCD system to the level of a few parts in 100,000, and by using a prism system to compensate for atmospheric dispersion.					
20. DISTRIBUTION/AVAILABILITY OF ABSTRACT UNCLASSIFIED/UNLIMITED <input checked="" type="checkbox"/> SAME AS RPT. <input checked="" type="checkbox"/> DTIC USERS <input type="checkbox"/>			21. ABSTRACT SECURITY CLASSIFICATION Unclassified		
22a. NAME OF RESPONSIBLE INDIVIDUAL Henry R. Radoski			22b. TELEPHONE NUMBER (Include Area Code) (202) 767-4906		22c. OFFICE SYMBOL NP

DD FORM 1473, 83 APR

EDITION OF 1 JAN 73 IS OBSOLETE.

UNCLASSIFIED

SECURITY CLASSIFICATION OF THIS PAGE

MATTHEW J. KERPER

Chief, Technical Information Division

1.0 ABSTRACT

Speckle interferometry has been carried out during the last year with a charge-coupled device (CCD) imaging system. The emphasis of this project has been to minimize all systematic differences that arise between the images of stars in a binary star system and a reference calibration star in order to resolve a previously unresolved binary star system. Systematic errors have been minimized to the level of parts in 10,000 in the power spectrum of a stellar image. This was accomplished by using a 64x64 pixel area near the readout amplifier to minimize charge smearing, by stabilizing our CCD system to the level of a few parts in 100,000, and by using a prism system to compensate for atmospheric dispersion.

For a second project, a procedure has been developed to separate overlapping images of galaxies in crowded fields and to make visible underlying structure. By modelling and subtracting away successively fainter and fainter objects and repeating this to achieve self-consistency, each object and the underlying structure can be made visible. It is expected that this technique is applicable to other problems.

For a third project, preliminary experiments have been carried out to test a technique to compensate for variations in absorption or emission at radio frequencies in the Earth's atmosphere. For this technique, two frequencies are used for simultaneous observations; one is used to correct the other statistically.

2.0 PRIMORDIAL HELIUM, THE RESOLUTION OF THE BINARY STAR SYSTEM μ -CASSIOPEIAE

The primordial helium abundance, the mass fraction of helium produced in the big bang, is of interest for several reasons. It can be used to set an upper limit on the cosmological mass density of baryons and to set an upper limit on the number of neutrino types. In addition, it is a fundamental variable in a variety of problems ranging from a detailed understanding of the early universe to the solar neutrino problem.

The thesis topic of James Haywood is to determine the helium abundance of the old binary star system μ -Cassiopeiae. Because μ -Cassiopeiae is an old stellar system whose chemical composition is characteristic of the early galaxy, its helium abundance should be characteristic of the primordial abundance. Enough information is available about the orbit of the binary system so that the masses of the stars and the helium abundance can be determined with one accurate measurement of the separation between the components. The observational problem is a difficult application of the technique of speckle interferometry; the ratio of intensity of the two stars differ by more than a factor of 100 in the visible part of the spectrum and the stars are close together. The expected separation between the components lies in the range of between about 0.5 to 1 arc second.

The resolution of the components of μ -Cassiopeiae is difficult not only because of the limited signal-to-noise ratio in the speckle exposures, but also because of the presence of small systematic differences between the images of μ -Cassiopeiae and the images of a nearby single calibration star.



Dist	Avail and/or Special
A-1	

The technique is to use the image of the single calibration star as a template to fit each of the components of the binary since all images are expected to have the same shape. But the problem is that any distortion in the image of the calibration star relative to the bright component of μ -Cassiopeiae tends to obscure the image of the faint companion star in the fitting process. Thus, at this time, our success with this project seems to be completely dependent upon understanding and removing all systematic differences between the images of the binary components and the reference calibration star.

There are two distinct classes of possible systematic errors, those due to the imaging system and those due to the atmosphere. At the present time we have demonstrated that the systematic differences among the images that we have observed are not due to the charge-coupled device (CCD) imaging system. There could be a variety of effects arising because of the microscopic structure of the CCD. We shall mention two of the possibilities. The direction of the saw cut to slice the silicon wafer from which the CCD is constructed can be determined by looking very closely at stellar images. This does not cause us any problems because our CCD is very stable, at the level of a few parts in 100,000, and, therefore, is reproduceable. The second effect is due to the incomplete transfer of charge in the horizontal and vertical direction in the CCD. This second problem is potentially very troublesome because it introduces a non-linearity into the system. The amount of charge lost due to incomplete charge transfer is about the same, relatively independent of the amount of signal charge present in a pixel: it takes a certain amount of charge to fill a trap independent of the signal amplitude. Our solution to this problem is to use a 64×64 area closest to the readout amplifier located on the CCD. Then, the number of charge transfers is minimized to the extent that the smearing is not observable.

The systematic difference between each component of the binary and the calibration star appears to be entirely due to differential refraction in the Earth's atmosphere. To correct for differential refraction, we have built a prismatic corrector which is inserted into the CCD optical train. Also, a program was written to determine prism angles as a function of the hour angle and declination of the star observed. Using this corrector, it was possible to resolve a binary star system with a zenith distance larger than 50 degrees having a separation of 0.75 arc seconds and a ratio of intensity between the components of 10 using only 32-20 millisecond exposures.

The prismatic corrector was only used during the last of our three observing runs during this reporting period. For this run we saw a large reduction in the size of the systematic differences between images. Though the prisms were adjusted every 10 minutes, which appears to be often enough based on our calculations, some small residual differences were still observed between images. However, when images were matched so that both binary and calibration star were observed under similar atmospheric conditions, they had similar distortions. It was found that the power spectra of these stellar images looked very similar even at the point at which the power had dropped (in the high frequency wings of the curve) to 5/10,000 of the peak value. The important conclusion of this part of the work is it appears that if we adjusted the prisms more frequently than every ten minutes, we would reduce the systematic differences between images to a negligible level.

Regarding our progress on μ -Cassiopeiae, we have made significant progress understanding how to treat CCD readout noise which has improved the quality of the data reduction procedure. Now we are finding a binary companion in the image of μ -Cassiopeiae at the expected position at a reasonable separation. However, at this time it would be premature to say any more about these preliminary solutions other than that the faint companion star to μ -Cassiopeiae has an intensity of less than one percent of the primary in the infrared.

3.0 THE METRIC ANGULAR DIAMETER COSMOLOGICAL TEST

Work has been progressing on the metric angular diameter versus redshift cosmological test. This is a test to determine whether the universe will expand forever or will one day collapse. The discriminant between these possibilities is the curvature of space. To measure curvature, the angular diameter of a class of galaxies having the same intrinsic size is observed as a function of redshift or distance. The variation of angular diameter as a function of redshift contains the curvature information.

In order to carry out the angular diameter test, we have proposed to carry out our observations at the same proper wavelength independent of redshift. Thus, we shall not have to make the standard "K" correction because our observations are made at the same proper wavelength as seen in the rest frame of the observed galaxy rather than at the same laboratory wavelength as has been the case in the past. In this regard, during the past year we have completed the photometric calibration of our CCD system. Our system uses a set of 1000 Angstrom bandwidth filters one of which is chosen to match the redshift of the galaxy of interest. Six continuous nights of photometric observing conditions at Mc Graw-Hill Observatory in June of last year gave us sufficient data to show that we can do photometry to 0.0075 magnitudes rms (0.75 %). Indeed, it is likely that we are limited not by the precision of our CCD measurements, but by the errors in the published standard star magnitudes and spectrophotometric data. In this regard, we confirmed a systematic error in the published spectrophotometry of Vega, finding that the published R and I magnitudes of that star are too faint by 0.08 magnitudes.

One of the issues that we have been concerned with for the angular diameter test is the constancy of the functional form of the surface brightness distribution of the light of a galaxy. Since our definition of the metric angular diameter is dependant on the surface brightness distribution of the galaxy light, it is essential that the galaxy light distribution does not change in a systematic way with distance. Though we have argued on physical grounds that we do not expect this to be the case, it is clear that good observational data must be used to justify this important assumption. We now have that data. A preliminary look at the color gradients calculated from exposures at 6000 and 8000 Angstroms in three clusters of galaxies at three different redshifts out to 0.175, showed that all appeared similar and had gradients which made their centers redder by only 0.1 to 0.2 magnitudes. This result has given us confidence that systematic effects depending on the stellar populations in clusters at different redshifts will not be a problem for the redshift-diameter cosmological test. The investigation of color gradients in clusters of different richnesses can also yield information

on the details of galaxy accretion and we are currently analyzing several clusters with this purpose in mind. We also have exposures at two wavelengths for galaxy M37. Not only will we obtain a color gradient of the galaxy, but by using our modeling and subtraction technique, we will obtain colors of the globular clusters very close to the center. The partially reduced data show about 200 globular clusters within 2.5 arc minutes of the center, many of which have never been studied.

In fact, what we have developed is a technique of more general applicability which is useful in any crowded field of objects. The basic principle is applicable to any linear detector--the principle is that of superposition. It is applied by first modeling and subtracting the brightest object in the field and then the second brightest object, etc. Then the process is repeated until a self-consistent solution is obtained. With some of the clutter removed the first object can be modeled more precisely, and removed more accurately and the process may be repeated on successively fainter objects. In this way, very faint objects originally obscured by much brighter objects can be made visible. During the past year two of our programs were selected for recognition by the University's QUEST program.

4.0 MASSIVE HALOS OF SPIRAL GALAXIES

In March, D. Hegyi presented an invited paper on the subject, "Are Massive Halos Baryonic?" at the joint session of the Moriond Astrophysics Meeting and the Moriond Particle Physics. (This meeting was supported, in part, by NATO.) The paper describes the arguments which show why it is unlikely that halos of spiral galaxies are composed of baryonic matter. New arguments were presented against halos being composed of planets or asteroids. D. Hegyi was also invited to present similar talks in June at the meeting in Rome on "Dark Matter" and, in November, at Fermilab in Batavia, Illinois.

Relevant to this subject, we have completed a study of the halo of galaxy NGC4565 with the purpose of setting a more stringent upper limit on the amount of visible light present. Ten hours of CCD integration on this object and a least squares fit to the expected $1/r$ law for a halo give an upper limit which is about 4 times smaller than that previously reported. The lower limit to the mass-to-luminosity ratio is thus 4 times higher and argues more strongly against the halo being made up of baryonic matter.

5.0 THE CHARGE-COUPLED DEVICE IMAGING SYSTEM

Our major hardware improvement during the past year is a stainless steel fill tube assembly for the CCD dewar. During past observing runs we have experienced vacuum leaks from the soft solder and silver solder joints of this assembly. The extreme temperature changes which the solder joints have to undergo each time the dewar is filled inevitably produce vacuum leaks. Our solution is to use welded stainless steel joints in an arrangement which allows operation in the normal orientation (at the cassegrain focus) or in an inverted position (at the prime focus). This new assembly has functioned without fault for the past three observing runs.

Our CCD electronics was improved by an increase in the stability of the first amplifier through a redesign of the buffer which controls the voltage offset. This change and a reworking of the CCD heater control circuit has given us a stability of the bias level over a night's observations of about ten electrons rms.

For our NOVA computer which controls the operation of the CCD, we have written additional programs in FORTH and assembler to aid in the acquisition of spectroscopic data. These programs allow real time focusing of the telescope and spectrograph on a selected comparison spectrum line.

In June, D. Gudehus presented an abstract on the "Construction of a CCD System" at the 162nd American Astronomical Society Meeting. Copies of this and the paper on halos follow the grant summary.

6.0 THE SMALL SCALE ANISOTROPY OF THE COSMIC MICROWAVE BACKGROUND

Finally, with M. Kutner of Rensselaer Polytechnic Institute, we have made observations at the 140 foot telescope in West Virginia on the small scale anisotropy of the 3 degree cosmic background radiation. Observations were carried out with a new technique to correct for rapid variations in atmospheric transparency. We observed at two frequencies simultaneously, 1 cm and 3 cm, using the 1 cm data to correct for fluctuations at 3 cm. NRAO is currently installing a beamsplitter on the 140 foot telescope so that the path through the atmosphere of the 1 and 3 cm beams will be more exactly overlapping. With the new beamsplitter both beams will have the same paths through the atmosphere and will have the same fluctuations.

ARE MASSIVE HALOS BARYONIC?

Dennis J. Hegyi

Department of Physics
University of Michigan
Ann Arbor, Michigan

ABSTRACT

The problems with massive halos being composed of baryonic matter are discussed. Specifically, a halo composed of either gas, snowballs, dust and rocks, low mass stars, Jupiters, dead stars or neutron stars is shown to be unlikely. Halos could be composed of black holes less than $100 M_{\odot}$ if they, unlike the stars in this mass range, are extremely efficiently accreting or primordial. At present, however, particles from supersymmetric theories appear to offer the most interesting possibilities as the constituents of halos.

I. INTRODUCTION

Spiral galaxies are surrounded by halos, large amounts of sub-luminous or non-luminous matter. These halos are approximately spherical in shape and may extend out to distances as far as ten times the optical radius of a spiral galaxy.

The supporting evidence for halos is quite compelling. Using dynamical arguments based on the rotation curves of spiral galaxies, it is possible to accurately determine the halo mass as a function of galactic radius. Also, a number of independent arguments require that halos be approximately spherical. Based on the information available about halos, it is not difficult to show that halos contain about 10-100 times the mass in the disks of spiral galaxies, and consequently, contain a significant fraction of the cosmological mass density.

In contrast to the definite statements that can be made regarding the existence of halos, very little can be said about the exact nature of the halo mass. At present, it appears that the most direct way to determine the composition of the halo mass is to show what halos cannot contain.

In the present investigation we argue that halos are not composed of baryons. Our approach will be to show the problems associated with the following types of baryonic matter: gas, snowballs, dust and rocks, Jupiter-like objects, low mass stars, dead stars and neutron stars. It appears very difficult to avoid the problems that we shall present if halos are baryonic. We shall discuss a model in which it is claimed, a primordial halo composed of gas can be converted into Jupiters, and show that it is not self-consistent.

Though not baryonic, black holes are a possible constituent of halos. If halos are composed of black holes they must be extremely efficiently accreting or primordial. Aside from the possibility of efficiently accreting black holes, we expect the cosmological baryonic abundance to be low at the time of nucleosynthesis. We shall briefly discuss the current situation regarding the observed nuclear abundances in terms of cosmological production in a low baryon density universe.

One of the earliest discussions of massive halos surrounding spiral galaxies was given by Hohl (1,2). He found his models of spiral disks to be unstable with respect to the growth of long wavelength modes, and as a result, the disks tended to develop into bar-shaped structures within about two revolutions. Hohl was able to stabilize his models by adding a fixed central force which he identified with a halo population of stars and the central core of the galaxy. Kalnajs (3), considering only exact solutions for infinitely thin spiral disks, explored ways of stabilizing the initially cool rotational state. Perhaps his most interesting result was that by embedding the spiral disk in a uniform density halo, stability could be obtained.

The possibility that spiral galaxies might be surrounded by massive halos was emphasized by Ostriker and Peebles (4). Using a 300-star galactic model they studied the instability of spiral structure to the development of bar-like modes. The onset of instability was reached when t , the ratio of the kinetic energy of rotation to the total gravitational energy, increased to a value ~ 0.14 . From a literature survey, the authors concluded that for systems ranging from fluid Maclaurin spheroids to flat galactic systems with 10^5 stars, the critical value for the onset of instability appears to be $t \approx 0.14$. Two different ways were suggested to stabilize the spiral structure, a hot disk population with radial orbits and a hot spherical halo. From a

variety of arguments, it is now known that the halo mass distribution is spherical.

The strongest observational evidence supporting the existence of massive halos is dynamical. The rotation curve of a galaxy must satisfy the criterion that in equilibrium the inwardly directed gravitational force must balance the outwardly directed centrifugal force. Rotation curves of galaxies have been obtained by both optical and radio techniques (5-11). Data obtained on more than 50 spiral galaxies reveal symmetric rotation curves which support the equilibrium condition

$$M_r = \frac{K}{G} v^2 r . \quad (1)$$

where M_r is the mass within radius r , K is a constant ranging from $2/\pi$ for a thin disk to unity for a spherically symmetric mass distribution, G is the gravitational constant, and v is the circular rotational velocity at galactic radius r . The observations show that v is a constant independent of r , and, as may be seen from eq. (1), $M_r \propto r$.

Beyond about 50 Kpc it is difficult, typically, to observe rotation curves, and binary galaxies (12,13) have been used to sample the halo mass distribution at large radii. Unfortunately there are a variety of selection effects which binary galaxies are subject to and it has not yet been possible to untangle these effects sufficiently to unambiguously interpret the results (14).

As already mentioned, several arguments have been used to show that the mass distribution of halos is spherically symmetric. The persistence of warps in spiral disks (15,16), star counts (17), and the scale height of stars perpendicular to spiral disks (18,19), all indicate relatively spherical halos, i.e. with aspect ratios close to unity.

II. EVIDENCE AGAINST NONBARYONIC HALOS

Much of the discussion about nonbaryonic halos has been presented elsewhere by Hegyi and Olive (20). Here we shall summarize parts of that discussion and amplify other parts. Before starting, however, we define a "standard halo" which we shall need to evaluate a variety of properties of baryonic halos. For this halo, $M_r \approx 10^{12} M_\odot$ in a radius of 100 kpc.

First we consider a halo made of gas. In a cold gaseous halo, particles moving on radial orbits would quickly collide with other gas particles and collapse on a gravitational

timescale $\tau_c = (3\pi/32G\rho)^{1/2} \approx 5 \times 10^8$ yrs. Since halos must persist for 10^{10} years, they must be in hydrostatic equilibrium and they must be hot. Our standard halo, if it were gaseous, requires an equilibrium temperature of $T_{eq} \approx 2 \times 10^6$ K which is sufficiently hot to violate the upper limits on the X-ray background by a factor of 20. The X-ray emissivity is sensitive to Ω_{halo} , the fraction of the critical density contained in halo. We use $\Omega_{halo} > 0.05$ (21).

A halo of snowballs will not be stable on a cosmological timescale. Snowballs, consisting primarily of hydrogen, are distinguishable from Jupiters because they are bound electrostatically. It turns out that the binding energy of a hydrogen molecule to solid hydrogen is sufficiently small so it easily escapes, even when the temperature of the snowball at 3°K, the temperature of the present cosmic background radiation. In fact, halos must have formed when the temperature of the cosmic background radiation was over 7°K; since halos are composed of non-interacting particles and cannot evolve to higher densities, they must have formed when the density of the universe had a density about equal to the present density of halos.

The argument against a halo of snowballs requires two steps. Based on laboratory measurements on solid hydrogen, its vapor pressure at 3°K has been found to be about 9×10^{-12} mm (22). This is high enough so that it is possible to show that there is no equilibrium between the solid and gaseous phase of hydrogen. The second part of the discussion involves the rate at which molecules evaporate to reach equilibrium. The time for evaporation (23) of a H_2 molecule (molecules rather than atomic hydrogen, will leave the snowball preferentially because their binding energy is lower) is

$$\tau_{ev} \sim [\nu_0 e^{-b/kT}]^{-1} . \quad (2)$$

The evaporation time is the inverse of the product of two terms: a Boltzmann factor which is the probability of a system attaining the escape energy, and an attempt frequency, the number of times per second that the system strikes the barrier. The reader is referred to (20) for more details. Here we report that at 3°K, the evaporation time per molecule is less than 10^{-8} seconds.

Next we consider a halo composed of dust and rocks, i.e. metals. A halo made of metals would contain a factor of about 50 times the mass of the disk of a spiral galaxy. The factor of 50 arises as the ratio of $\Omega_{halo}/\Omega_{disk} \geq .05/.001 \approx 50$. The problem is that if even a very small fraction of the halo mass mixed with the disk it would lead to a large metal abundance in the disk. Since the halo is believed to have formed before the disk and since there are disk stars with metal abundances $Z \sim 10^{-5}$,

this implies that less than about one part in 5×10^6 of the halo mixed with the disk gas. It is difficult to believe that the halo could be composed of metals without contaminating the disk at such a low level.

The next possibility that we consider is a halo composed of low mass stars or Jupiters (24), that is, objects which are gravitationally bound with $m \leq 0.08 M_0$ which do not have high enough central temperatures to support nuclear burning. By making observations of the surface brightness of the halo, it is possible to set limits on the mass in low mass stars. If a connection can be established between the nuclear burning stars ($M > 0.8 M_0$) and the Jupiters, then by establishing constraints on the luminous portion of the initial mass function, constraints are simultaneously set on the non-nuclear burning portion of the initial mass function.

To connect the luminous and non-luminous parts to the halo initial mass function, a single power law relation has been assumed. The justification for this assumption is that the physics which affects the lower mass limit for nuclear burning is independent of the physics which governs gravitational collapse and it would be a considerable coincidence if these two mass scales coincided. Nuclear burning depends on the fine structure constant, α , and the strength and range of strong interactions while the physics of gravitational collapse depends on α and the gravitational constant, G . Since the assumption that the halo initial mass function is a single power law is the strongest assumption in this manuscript, we shall return to this subject to present other supporting evidence and discuss the substantial problems that must be overcome to seriously consider a radically different initial mass function, namely a halo of Jupiters with negligible mass in nuclear burning stars.

As we shall show, the mass-to-light ratio, M/L , of a halo is a function of the slope of the initial mass function, x , and the lowest mass condensation which forms gravitationally, m_{\min} , also known as the Jeans mass. The initial mass function is defined by

$$\phi_m = A m^{-(1+x)}, \quad (3)$$

where ϕ_m is the number of stars per unit mass per unit volume of the halo. In general, A and x will depend on the mass range considered. The total mass density in stars and Jupiters, ρ_m , is

$$\rho_m = \int_{m_{\min}}^{m_G} m \phi_m dm, \quad (4)$$

which, using eq. (3) may be found to be,

$$= \frac{A}{1-x} [m_G^{1-x} - m_{\min}^{1-x}] . \quad (5)$$

Here, m_G is the mass of a giant which is taken to be $m_G \approx 0.75 M_\odot$ and for the present argument, we neglect the small fraction of the mass contained in more massive objects.

Using the initial mass function, the luminosity density of the halo, ρ_L , may be seen to be,

$$\rho_L = \int_{m_0}^{m_G} L_m \phi_m dm + L_G . \quad (6)$$

For

$$L_m = c m^D , \quad (6a)$$

$$\rho_L = \frac{Ac}{D-x} [m_G^{D-x} - m_0^{D-x}] + L_G , \quad (7)$$

where L_m is the luminosity of a star of mass m , and c and D are constants chosen for a particular spectral band. The lower limit of integration, m_0 , in eq.(6), the lower limit for nuclear burning, has been taken to be $m_0 = 0.08 M_\odot$ (25). The quantity, L_G , is the light due to giants. Since observational constraints are available in the I and K Johnson spectral bands for the halo of the edge-on spiral galaxy NGC 4565 we shall evaluate ρ_L in these bands. The data of Gunn and Tinsley (26) in the range $0.05 M_\odot$ to $0.8 M_\odot$ have been fit with the power law in eq.(6a). For the luminosity in the I band, $L_{m,I}$, $c = 1.49 \times 10^{-3}$ and $D = 2.71$ and, correspondingly, for $L_{m,K}$, $c = 3.12 \times 10^{-2}$ and $D = 2.11$ where mass is expressed in solar units and in each spectral band, the luminosity equals unity for a zero magnitude star.

To express the contribution of giants to the surface brightness we have used the method described in Tinsley (27). Since Tinsley discussed a metal abundance $Z = .01$, we corrected the Tinsley models using the calculations of Sweigart and Gross (28). Fitting the later calculations (for $m = .7 M_\odot$, $Y = .30$) for the change in main sequence lifetime as a function of Z , the correction to the lifetime was found to be $\propto \exp[23.6Z - .286]$, that is, increasing Z increased main sequence lifetimes. Also, it may be seen that this factor is equal to unity for $Z = 0.01$. For these calculations we have used $Z = 10^{-5}$, a value appropriate to halo stars. Lifetimes for smaller metal abundances are not changed appreciably.

To calculate M/L for the halo of NGC 4565, we shall use $M/L = \rho_m/\rho_L = \sigma_m/\sigma_L$, where σ_m and σ_L are the projected mass and luminosity density. It is necessary to evaluate the projected halo mass density in terms of the 21 cm rotational velocity 253 km/s (29) and the maximum extent of the halo, R_{\max} . This may be seen to be

$$\sigma_m = \frac{v^2}{2\pi G r} \tan^{-1} \sqrt{\left(\frac{R_{\max}}{r}\right)^2 - 1} \quad (8)$$

at galactic radius r . The distance to NGC 4565 is unlikely to be larger than 24 Mpc, and since the rotation curve has been observed out to 11.6'', $R_{\max} = 31$ Kpc. Using eq.(8) and eq.(7), it may be seen that M/L for the halo is only a function of x and m_{\min} .

We now turn to the observational data on the surface brightness of the halo of NGC 4565. Data taken with the annular scanning photometer (30) in the Kron 1 band has been discussed by Hegyi (31), see Figure 1. That data has been transformed to the Johnson system and expressed in solar units. A least squares fit to that data using the functional form $\sigma_L = a/r + b$ has been performed. (This functional form assumes that R_{\max} is large compared to r so that the \tan^{-1} function in eq. 8 reduces to $\pi/2$.) A 2σ lower limit to σ_m/σ_L expressed in solar units in the Johnson I band is

$$M/L_I > 60 M_\odot/L_{\odot,I} \quad (9)$$

Observations in the K band have been made by Boughn, Saulson, and Seldner (32) using a chopping secondary. Their 2σ lower limit is

$$M/L_K > 38 M_\odot/L_{\odot,K} \quad (10)$$

We shall now determine whether the available observational and theoretical constraints on x and m_{\min} can accommodate the limits on M/L in eqs. (9) and (10). The strongest constraints on x , derived from the observation of spectral features (26) and the initial mass function in the solar neighborhood (33) require $x < 1$ at the 2σ level. Also there is no data in conflict with $x < 1$. Photometric data ranging from globular clusters to elliptical galaxies can be fit using the weaker constraints $x < 1.35$, by a single free parameter, the metal abundance (34,35).

Constraints on m_{\min} , the smallest mass to collapse gravitationally (36,37,38), have a lower limit of $> 0.007 M_\odot$. A more recent calculation (39) in which new reactions to form

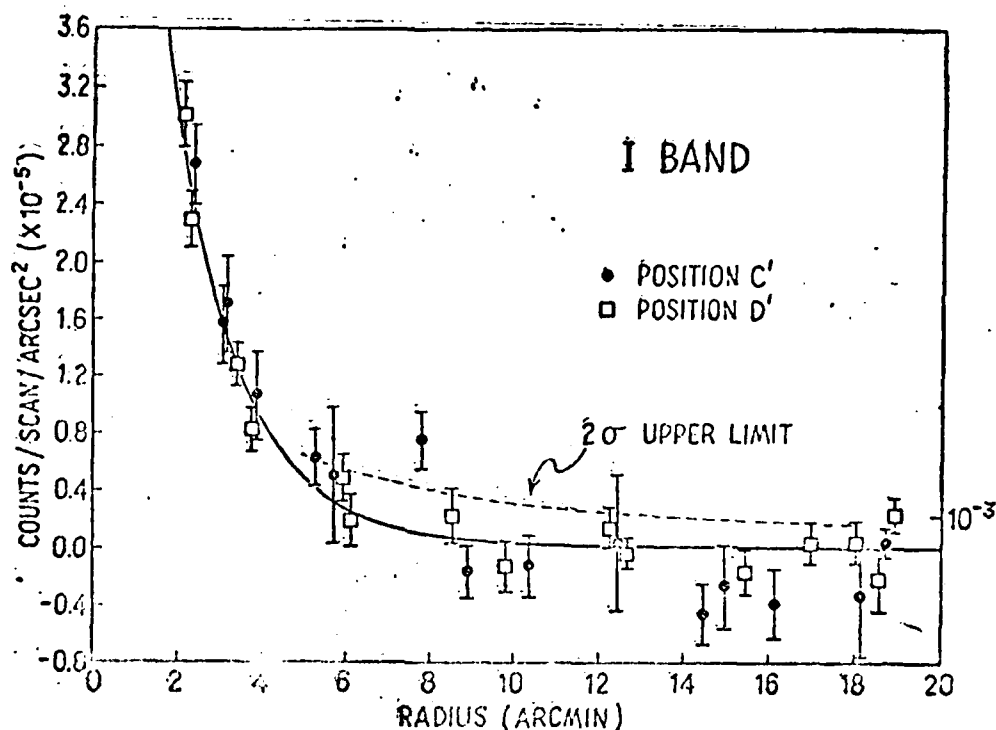


Figure 1. The measured surface brightness of the halo of NGC 4565 versus galactic radius. Positions C' and D' are two symmetric scanning positions. The curve fitted to the data is the de Vaucouleur's surface brightness law and the 2σ upper limit to the data is labelled. [1 count/scan/arc sec² $\times 10^{-5}$ is 25.34 mag I_{Kron}.]

molecular hydrogen are considered, requires $m_{\min} > 0.004 M_{\odot}$. That result was found for optically thin clouds. An equally forceful position has been presented in which it is argued that the first objects to form have $m_{\min} > 1500 M_{\odot}$.

If we choose $m_{\min} = 0.004 M_{\odot}$ and find x to satisfy the I and K band NGC 4565 observations, we find $x > 1.6$ and 1.7 respectively. On the other hand, if we choose $x < 1$ and try to find the allowed range for m_{\min} , we find no solution. It is not possible to put enough mass in the halo for this x without violating the surface brightness observations. For $x = 1.35$, we find $m_{\min} < 2 \times 10^{-4} M_{\odot}$ at least a factor of twenty below the calculated lower limit on m_{\min} . These are the problems if one chooses to consider a single power law initial mass function and a halo of stars and/or Jupiters.

There are some observations which have a bearing on our assumption of whether the initial mass function is a single power law below the nuclear burning cutoff. Probst and O'Connell (41) argue that the initial mass function in the solar neighborhood does not even rise as steeply as a single power law for stellar masses less than $0.1 M_{\odot}$. Instead the slope turns over, meaning that there is little mass contained in stars with $m < 0.1 M_{\odot}$. Since these results are based on stars with solar metal abundance, the conclusions are strengthened for stars which have lower metal abundances and which cannot cool as effectively.

Though we have argued that it seems reasonable to use a power law for the slope of the initial mass near $0.08 H_2$ and that any possible gravitational condensation of smaller mass would adhere to the same power law, let us now consider the possibility that only Jupiters formed. As a prototypical model, we shall consider the model presented at this conference by Professor Rees. In that model, a Jean's mass at recombination, $10^5 - 10^6 M_{\odot}$, cools and forms a very thin disk of thickness equal to the Jean's length of a $10^{-3} M_{\odot}$ condensation, that is, a Jupiter. Subsequently the disk fragments contributing $10^8 - 10^9$ Jupiters to the formation of a halo of Jupiters.

There appear to be two large-scale instabilities which the disk must avoid if Jupiters are to form: the tendency of the disk to form a bar, and the instability of a cool disk to form massive condensations which are a significant fraction of the total disk mass (42). We shall discuss the second instability using the Toomre stability criterion.

The basic kinematic criterion for stability is that the time for a blob of material to orbit the disk, t_{orb} , should be longer than the time for a pressure wave or sound wave to cross the disk, t_s . Writing $t_{orb} \sim r/v$ and $t_s \sim r/c_s$, we have

$$t_{orb} > t_s \quad (11)$$

leading to

$$r/v > r/c_s \quad (12)$$

or

$$v < c_s . \quad (13)$$

This is the condition that, for stability, the orbital velocities be less than the individual particle velocities. Adding the dynamics, namely in equilibrium, the following condition for circular motion must be satisfied,

$$v^2/r = GM/r^2 . \quad (14)$$

For a disk with mass per unit area, σ , $M \sim \pi \sigma r^2$, then substituting for M in eq. (14) and multiplying by r , we have

$$v^2 = \pi G \sigma r . \quad (15)$$

Substituting this result into eq. (13) leads to

$$\pi G \sigma r < c_s^2 \quad (16)$$

The speed of sound is $c_s^2 \sim KT/m_p$. Also, from the Jeans mass condition we have

$$GM_J/r_J \sim KT/m_p . \quad (17)$$

where M_J is the Jeans mass and r_J is the Jeans length. Substituting eq. (17) into eq. (16), it may be seen that

$$\pi G \sigma r < c_s^2 \sim GM_J/r_J \quad (18)$$

or

$$\pi \sigma r r_J < M_J . \quad (19)$$

If we write the thickness of the disk, t , in terms of the radius of the disk, r , then $t = \epsilon r$. With $t = r_J$ and $M \sim \pi \sigma r^2$, we have

$$\epsilon M < M_J . \quad (20)$$

From the numbers required by the model, that is, dividing a $10^5 M_\odot$ object into $10^{-3} M_\odot$ objects or 10^8 Jupiters, it may be seen that the ratio t/r required for a disk of thickness equal to the Jeans length of a Jupiter is $\sim \sqrt{10^{-8}} = 10^{-4}$. Using this value for ϵ on the left hand side of eq. (20) yields $\sim 10 M_\odot$, while the desired Jeans mass is $10^{-3} M_\odot$. The inequality is not satisfied by a factor of 10^4 . That is, such thin disks are unstable and form $\sim 10 M_\odot$ objects, not Jupiters. An alternative interpretation is that a disk which is not enough for stability is too hot to allow low mass gravitational condensations to develop.

The halo cannot be made of stars which have an initial mass greater than $2 M_\odot$. Such stars either evolve to white dwarfs with mass $\sim 1.4 M_\odot$ (43) or to neutron stars which also, coincidentally, have masses $\sim 1.4 M_\odot$. Taylor and Weisberg (44) have found two neutron stars with masses of $1.4 M_\odot$ to within 1% and all other neutron star mass determinations are consistent with $1.4 M_\odot$. Consequently, any star with initial mass greater than $2 M_\odot$ must

lose 40 per cent of its mass during evolution. The ejected mass cannot be hot because of previous arguments and it cannot cool and fall in the disk because there is too much mass to be contained. Also, since a significant fraction of the mass of the evolved stars, $> 10\%$, might be expected to be converted into helium and metals during evolution, problems similar to those raised by metallic halos could be present.

Though black holes do not have a well defined baryon number, we shall briefly consider them because if halos are not baryonic, they are evidently either composed of black holes or some weakly or very weakly interacting particles (see review by Joel Primack in this volume).

It appears unlikely that many black holes in the mass range $1-50 M_{\odot}$ formed in the halo. Stars in this mass range eject a considerable fraction of their mass. Unless the black holes can accrete virtually all their ejecta, problems similar to those with metallic halos arise. Black holes which are more massive than $100 M_{\odot}$ appear to be excluded by new observations (45), though they need to be confirmed. Thus, halos could be composed of black holes in the mass range $\sim 50-100 M_{\odot}$ (46) or they could be primordial.

Arguing by eliminating specific baryonic forms of matter is not the most persuasive way to argue that halos are not baryonic, but, unfortunately, we are unable to present a forceful positive argument eliminating baryons directly. In this context, it is worth considering the constraints that primordial nucleosynthesis places on baryonic halos, though we admit that there are strong assumptions implicit in the nucleosynthesis calculations.

In this context, we shall take the simplest point of view, namely, that all the dark matter in halos and rich clusters is either all baryonic, or not baryonic and see which conclusion, if any, the nuclear abundances favor.

A lower limit to the mass fraction of the closure density in baryons, Ω_b , may be obtained from the luminous matter in galaxies and could be as low as .001. The thermal X-ray fluxes from clusters of galaxies yield higher baryon abundances but do not exclude $\Omega_b \sim .001$. On the other hand if all the dark matter were baryonic, the mass content of halos and rich clusters would require a lower limit for the baryonic abundances to be, $\Omega_b \geq 0.1$.

The deuterium abundance of $\sim 1 \times 10^{-5}$ by mass does not favor either high or low baryon abundances. There are problems with both ranges. However, the deuterium abundance may not be well known (see Audouze this volume). The He^4 abundance is presently

observed to be in the range $Y \sim .22-.25$ (47). Since an observed helium abundance is an upper limit on the primordial abundance, and since $\Omega_b \geq .1$ requires $Y \geq .26$, the helium observations favor a low baryon abundance. The observed Li^7 abundance (48) is consistent with two abundance ranges, $\Omega_b \sim .001-.003$ and $\Omega_b \sim .01-.02$. It appears inconsistent with $\Omega_b \geq .1$. Taken together, the abundance data favors a low baryon abundance (49). A key test of the cosmological baryon abundance will be a new measurement of the primordial helium abundance which is independent of the possible systematic effects in the present spectroscopic measurements.

I would like to thank G. William Ford, Martin Rees, Alar Toomre and Scott Tremaine for useful discussions.

REFERENCES

1. Hohl, F. 1977, NASA TR R-343.
2. Hohl, F. 1975, in IAU Symposium No. 69, "Dynamics of Stellar Systems", ed. A. Hayli (Dordrecht, Neth: Reidel), pp. 349.
3. Kalnajs, A.J. 1972, Ap. J. 175, pp. 63.
4. Ostriker, J.P. and Peebles, P.J.E. 1973, Ap.J. 186, pp. 457.
5. Rogstad, D.H. and Shostak, G.S. 1972, Ap. J. 176, pp. 315.
6. Roberts, M.S. and Rots, A.H. 1973, Astr. Ap. 26, pp. 483.
7. Haschick, A.D. and Burke, B.F. 1975, Ap. J. (Letters) 200, pp. L137.
8. Roberts, M.S. 1975 in IAU Symposium No. 69, "Dynamics of Stellar Systems", ed. A. Hayli (Dordrecht, Neth: Reidel), pp. 331.
9. Sancisi, R. 1977, IAU Symposium No. 77, "Dynamics of Stellar Systems", ed. A. Hayli (Dordrecht, Neth: Reidel).
10. Krumm, N. and Salpeter, E.E. 1979, A.J. 84, pp. 1138.
11. Rubin, V.C., Ford, Jr., W.K., and Thonnard, N. 1978, Ap. J. (Letters) 225, pp. L107.
12. Turner, E.L. 1976, Ap. J. 208, pp. 304.

13. Peterson, S.D. 1979, Ap. J. 232, pp. 20.
14. Rivoio, A.R. and Yahil, A. 1981, Ap. J. 251, pp. 477.
15. Saar, E.M. 1978 in IAU Symposium 84, "The Large-Scale Characteristics of the Galaxy", ed. W.B. Burton.
16. Tubbs, A.D. and Sanders, R.H. 1979, Ap. J. 230, pp. 736.
17. Monet, D.G., Richstone, D.O. and Schechter, P.L. 1981, Ap. J. 245, pp. 454.
18. Van der Kruit, P.C. 1981, Ast. Ap. 99, pp. 298.
19. Rohlfs, K. 1982, Astr. Ap. 105, pp. 296.
20. Hegyi, D.J. and Olive, K.A., to be published 1983, Physics Letters.
21. Faber, S.M. and Gallagher, J.S. 1979, Ann. Ref. Astr. Ap. 17, pp. 135.
22. Johnson, V.J. 1960. "A Compendium of the Properties of Materials at Low Temperature (Phase I)", U.S. Air Force.
23. Hellenbach, D. and Salpeter, E.E. 1971, Ap. J. 163, pp. 155.
24. Dekel, A. and Shoham, J. 1979, Astro. Ap. 74, pp. 186.
25. Straka, W.C. 1971, Ap. J. 165, pp. 109.
26. Tinsley, B.M. and Gunn, J.E. 1976, Ap. J. 203, pp. 52.
27. Tinsley, B.M. 1976, Ap. J. 203, pp. 63.
28. Sweigart, A.V. and Gross, P.G. 1978, Ap. J. Suppl. 36, pp. 405.
29. Krumm, N. and Salpeter, E.E. 1979, A.J. 84, pp. 1138.
30. Hegyi, D.J. and Gerber, G.L. 1977, Ap. J. (Letters) 218, L7.
31. Hegyi, D.J. in Proceedings of the Moriond Astrophysics Meeting (ed. J. Andouze, P. Crane, T. Gaisser, D. Hegyi, and J. Tran Thanh Van) Frontiers, 1981, pp. 321.

32. Boughn, S.P., Saulson, P.R. and Seldner, M. 1981, Ap. J. (Letters) 250, pp. L15.
33. Miller, G.E. and Scalo, J.M. 1979, Ap. J. Suppl. 41, pp. 513.
34. Aaronson, M., Cohen, J.G., Mould, J. and Malkan, M. 1978, Ap. J. 223, pp. 824.
35. Frogel, J.A., Persson, S.E. and Cohen, J.G. 1980, Ap. J. 240, pp. 785.
36. Low, C. and Lynden-Bell, D. 1976, M.N.R.A.S. 176, pp. 367.
37. Rees, M.J. 1976, M.N.R.A.S. 176, pp. 483.
38. Silk, J. 1982, Ap. J. 256, pp. 514.
39. Palla, F., Salpeter, E.E., and Stahler, S.W. (preprint).
40. Tohline, J.F. 1980, Ap. J. 239, pp. 417.
41. Probst, R.G. and O'Connell, R.W. 1982, Ap. J. (Letters) 252, L69.
42. Toomre, A. 1964, Ap. J. 139, pp. 1217.
43. Chandrasekhar, S. 1935, M.N.R.A.S. 95, pp. 207.
44. Taylor, J.H. and Weisberg, J.M. 1982, Ap. J. 253, pp. 908.
45. Lin, D.N.C. and Faber, S.M. 1983 (preprint).
46. Carr, B.J., Bond, J.R. and Arnett, W.D. 1983 (preprint).
47. Pagel, B. 1982, Phil. Trans. of R.S. London 307, pp. 19.
48. Spitz, M. and Spitz, F. 1982, Nature 297, pp. 483.
49. Olive, K.A., Schramm, D.N., Steinman, G., Turner, M.S., Yang, J. 1981, Ap. J. 246, pp. 557.

function. These tails can lead to enhanced optical and uv line radiation. The energy loss of the beam is caused by the collisionless excitation of plasma waves, resistive heating and inverse Compton radiation. We will discuss the results of our calculations and some of their implications for interpreting observations of active galactic nuclei.

18.04 Measuring Magnetic Irregularities in Extragalactic Radio Sources. S. R. STABLER, U. Iowa. The observation of high fractional linear polarization in extragalactic radio sources is usually taken to be evidence for large-scale magnetic fields in these objects. Robert Laing has pointed out that high fractional polarization near the edge of a source and low percentage polarization near the center is consistent with a partially-ordered field configuration. In such a model, the magnetic field is completely random, but confined to planes which are tangent to the source boundaries. I have considered the transport of polarized synchrotron radiation in such a random medium. Expressions have been derived relating the observable autocorrelation functions of the Stokes parameters Q and U to the correlation functions of plasma density and magnetic fields in the source. The analysis predicts that the fractional linear polarization observed in the center of a lobe possessing a "Laing-type" magnetic field should be small but finite. This central fractional polarization is determined by the scale length of the irregularities. Beam dilution can result in a frequency dependence of the fractional linear polarization, even though there is no net Faraday rotation. The theory has been applied to dual-frequency observations of the radio galaxy J0100. The polarization characteristics of the south lobe of this source are consistent with an irregularity scale length which is a few percent of the lobe diameter.

18.05 Photometric History of the BL Lac Object B2 1308+326. S. L. JORDAN, Indiana U., W. Z. WISNIEWSKI, LPL, J. POLLOCK, Appalachian State, M. F. ALLER, H. D. ALLER, U. Michigan, W. A. STEIN, U. Minn.-- We have monitored the BL Lac object B2 1308+326 both photometrically (UBVRI) and photographically from 1976 until the present. During the same period we have also monitored this source in the radio (14.5 and 8.0 GHz). Finally we report two X-ray measurements made with the HEAO-2 satellite. The results of the optical and radio photometry show that B2 1308+326 is extremely active and variable. Although the B band photometry is not complete, there is a strong suggestion that this source bursts quasi-periodically on a time scale of approximately one year. The strengths of these outbursts are quite variable; we have observed the bursts to increase the B band flux density by factors ranging from 50% to 700%. Although the source also bursts in the radio, these bursts are in general not as pronounced as in the optical. There is only marginal evidence for a correlation between the optical and radio bursts. The two X-ray measurements were obtained during a quiescent period and a bursting period. The X-ray emission was significantly stronger while the source was bursting.

18.06 Wavelength-Dependent Polarization in B2 1308+326. M. L. SITKO, W. A. STEIN, U. Minn., G. D. SCHMIDT, U. of A. The BL Lacertae object B2 1308+326 has recently undergone a major flux outburst, reaching a visual magnitude $V = 14.8$ and an implied visual luminosity $\nu F_{\nu} = 2 \times 10^{47} \text{ erg s}^{-1}$ ($\nu = 545 \text{ THz}$, $H_0 = 50 \text{ km/sec/Mpc}$, $q_0 = 0$). During this outburst the polarimetric properties of its optical emission were monitored on two successive nights. On both nights a statistically significant dependence in the position angle of the polarization vector versus wavelength was observed. On one night θ_p differed in U and I photometric bands by 14 degrees (a 5 σ difference) while on the following night θ_p in these two bands differed by 17 degrees (a 5 σ difference). The temporal change of θ_p between the two nights was 10 degrees at all observed wavelengths, but the wavelength dependence was similar.

18.07 B2 1308+326 - A Super Massive Compact Object? W. A. STEIN, U. Minn., S. MCFYSON, IN. Univ., W. WISNIEWSKI, U OF A. During the period of early 1983 B2 1308+326 was observed during an outburst which, if interpreted in terms of an isotropic radiation flux and cosmological redshift of $Z = 0.996$ (Miller, French, and Hawley 1979, Pitts. Conf. on BL Lacertae Objects, p. 176), implies that it was the most luminous object in the universe known at that time. Interpretation of physical constraints on an observational status of this object over several years implies that it may be a super-massive compact object of $M = 10^{10} M_{\odot}$ and $R = 10^{10} \text{ cm}$. The light curve should be monitored at all wavelengths over the next decade in order to confirm or contradict this hypothesis.

Session 19: Instruments 0940-1100 (Wabasha South)

19.01 Construction of a CCD System.
D. H. GUDENUS AND D. J. HEGILL, Univ. of Mich.

We have constructed a CCD imaging system based on the RCA thinned chip (320 x 512 pixels) and have written software to do picture processing on a VAX/VMS 780 working in conjunction with a Grinnell image display system (GMR 270). Machine code for an AN2910 microprocessor is downloaded from a NOVA 3/12 minicomputer operating under FORTH. This convenience and the use of 15 transfer electrode potentials has given us great flexibility in optimizing the CCD's performance. The readout noise is 64 electrons and the threshold level for image trailing is 300 electrons in the center of the chip and zero for the area first to be read out. Blemishes are insignificant, fringing from night sky lines is not seen, residual images from a previous exposure are not present, and bleeding of charge from bright stars is not a problem. Flat field exposures on the dawn sky are consistent with each other to a few parts in 100,000 to a few parts in 1000 at worst, even when obtained on different nights. The device is linear to within our errors of measurement and the dynamic range is about 6000, being limited by our 14 bit ADC.

Supported by Air Force Grant AFOSR-80-0095